Title
Reconfigurable UWB Bandpass Filter with Flexible Notch Characteristics

Author
Dhwaj, Kirti

Publication Date
2014

Peer reviewed|Thesis/dissertation

University of California
Los Angeles

Reconfigurable UWB Bandpass Filter with Flexible Notch Characteristics

A thesis submitted in partial satisfaction
of the requirements for the degree
Master of Science in Electrical Engineering

by

Kirti Dhwaj

2014

2014

Abstract of the Thesis

Reconfigurable UWB Bandpass Filter with Flexible Notch Characteristics

by

Kirti Dhwaj

Master of Science in Electrical Engineering

University of California, Los Angeles, 2014

Professor Tatsuo Itoh, Chair

The thesis reports a compact tunable ultra-wideband (UWB) notch filter using hybrid microstrip and coplanar waveguide (CPW) structure. The tunable notch is implemented to filter out the wireless local area network (WLAN) channels from 5GHz to 6GHz. The proposed structure utilizes the resonance of open ended stubs to achieve transmission zeroes in the filter passband. Varactors and by-pass capacitors are then introduced for dynamic tunability of notch. Further, the electromagnetic decoupling of the two resonators leads to tunable bandwidth of notch. DC bias circuitry is implemented to control the varactor capacitances. Rejection levels up to 25 dB are attained using this technique while maintaining insertion loss levels below 2.5 dB in the passband. The reconfigurability of bandwidth is shown by maintaining a constant bandwidth of 150 MHz across the WLAN band for the notch. The filter achieves an excellent wide bandwidth (from 2.5 GHz to 8.5 GHz) using multimode-resonator (MMR) based topology which makes the filter one wavelength long at the central frequency.

The thesis of Kirti Dhwaj is approved.

Robert N. Candler

Diana L. Huffaker

Tatsuo Itoh, Committee Chair

University of California, Los Angeles

2014

To my mother . . .

for her unconditional love and support,

for making me possible.

And the golden fur-ball . . .

who has been watching over me from heavens above.

Table of Contents

List of Figures

List of Tables

Acknowledgments

I am extremely grateful to Professor Tatsuo Itoh, my graduate advisor and mentor for allowing me to pick the topic of choice for thesis work. He has been an invaluable source of knowledgeble inputs and a constant basis of inspiration for this work to come about. I would like to thank my professors from IIIT Allahabad - Neetesh Purohit and Ajay Singh Raghuvanshi for making the twin issues of distance and time appear trivial. I would also like to convey my gratitude to Deepak Nagarkoti and Shahram Mahadevi, my mentors at Broadcom and Silicon Laboratories, for having an indelible impact on my academic career.

It would be misleading to say that I would have been able to complete my research if it was not for my family and close friends, both in India and the United States, who not only stood by me during extremely tough times but also made sure my feet are, more often than not, planted firmly on the ground. Specifically, I would like to acknowledge Umang, Mukul Bharti, Achint, Mukul Gupta, Abde, Jacky Chan and Chris Curwen for continually reassuring me during the lean periods of my research. Last but not the least, I would like to thank Professors Diana Huffaker and Robert Candler for taking out their invaluable time to review and guide the manuscript to its final form.

CHAPTER 1

Introduction

1.1 Cognitive Radio for The Microwave Engineer

With the rapid proliferation of modern wireless devices and standards, the radio spectrum has become a prime commodity (Table 1.1). It is a common complaint that the radio spectrum is too crowded to introduce newer wireless services or indeed, faster services because of the lack of bandwidth. Although the congestion seems restrictive on the face of it, a spectrum monitoring exercise carried by FCC [for02] revealed that most of the designated bands are seldom occupied by their owners. For some bands, the usage was down to 10 per cent.

It is in this context that the concept of Software Defined Radio (SDR) becomes important. It refers to the characteristics of operating frequency, bandwidth and modulation being completely governed by software [Mit95]. The desired outcome is a radio capable of operating on any current or future standards by simply updating the software.

Cognitive Radio is an extension of the SDR, in the sense that the radio has "intelligence"

Standard	**Range (MHz)**	**Standard**	**Range (MHz)**
GSM 1800	1710-1880	Bluetooth	2402-2480
GSM 1900	1850-1990	IEEE 802.11a	515-5925
PCS (US)	1910-1990	IEEE 802.11b	2400-2497
IS -136	1850-1990	IEEE 802.11g	2400-2484
WCDMA FDD	1710-2110	UWB	3100-10600
WCDMA TDD	1850-2025	IEEE 802.16a	2000-11000

Table 1.1: Common wireless standards.

built into it. This entails developing a cognitive engine that could learn the RF environment from past observations and decide the correct communication standard, mode of operation and RF parameters [Mit00] [Mit06]. On a conceptual level, cognitive radio senses the spectral environment and adapts transmission parameters to dynamically resuse the available spectrum (Figure 1.1) [Wan09].

The question then arises: what can we as passive component engineers contribute to this technology? Adaptability in hardware is the bedrock for development of cognitive radio. In the commercial space, this would not only allow for efficient use of RF spectrum but also facilitate the integration of newer standards using a generalized reconfigurable RF front-end. It would save chains of hardware levels from being added to introduce new functionality in existing communication devices. In the military domain, standards-based approach might not hold but applications like mission based flexibility and

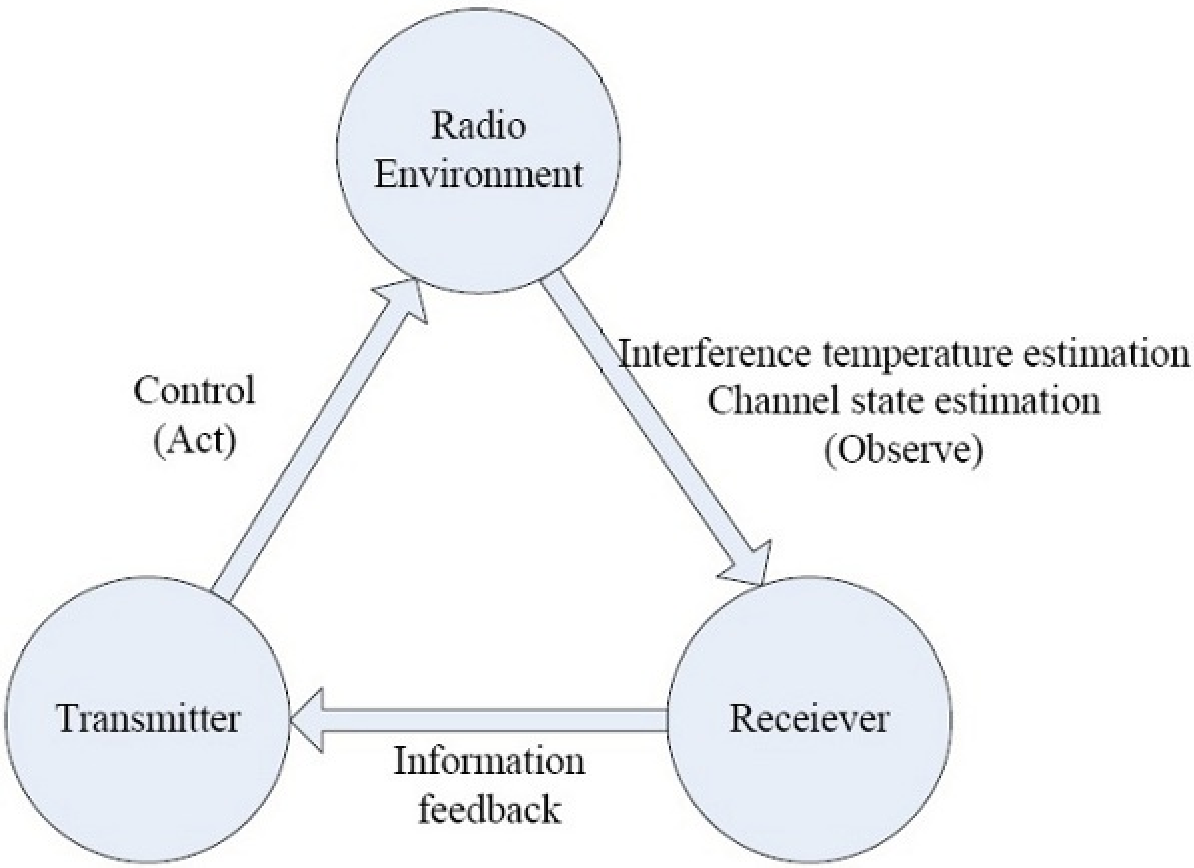

Figure 1.1: Cognitive radio cycle.

jamming mitigation offer a compelling incentive for hardware development[CNM14]. Also, change of hardware due to differences in standards is responsible for a massive stream of electronic waste [Sol13][RB10]. Telecommunication manufacturars can use the adaptable nature of RF front ends to create generalized systems with longer lifetimes.

While the use of FPGA has shown that a universal digital system for various radio technologies is possible, no such capability exists in the microwave domain. For achieving tunability in a RF front end, reconfigurability can be ascribed to components such as low noise amplifiers, filters, antennas etc. This thesis focuses on adaptive filtering for cognitive radios. From the perspective of a filter designer there is no difference between a design for SDR or a cognitive radio. The filter is responsible for the tuneability of frequency and bandwidth. Other parameters which become consequential for migration from one standard to another include linearity and power handling but they won't be handled in this thesis.

1.2 Ultra-Wideband (UWB) Cognitive Radio

Since the release of ultra-wideband (UWB) frequency spectrum (3.1 to 10.6 GHz) by the Federal Communications Commission [RO02], the UWB bandpass filter (BPF) has received considerable attention from both industry and academia[HL08]. UWB systems offer a fair number of advantages:

(i) Capability to support high data rates and number of users.

(ii) Enhanced capability to penetrate through obstacles.

(iii) Better ranging at centimeter level.

(iv) Support development of small sized and processing powered devices.

(v) Low electromagnetic radiation. For example, FCC limits the indoor UWB systems to a maximum power transmission of -41dBm/MHz.

The above qualities make UWB systems a favorable alternative for a variety of potential applications. Some of them are:

(i) *Computer Peripherals*: It is possible to exchange range with data rate by aggregating more energy per datum. High-data rate UWB may enable multimedia services to be transmitted wirelessly to devices like wireless monitors.

(ii) *Medical Devices* : UWB is the best candidate for wireless body area network (WBAN) applications. WBAN consists of miniaturized, low power (<100μW) biosensers, seamlessly placed or implanted in human body to provide better healthcare. Because of extremely low power consumption, the UWB technology offers a very practical solution to this application which no other narrowband service does. Also, the UWB system architecture manifests considerable complexity on the receiver side, thereby ridding the implanted sensor of much hardware and making it small.

(iii) *Radar Applications* : The extremely narrow pulse-width (usually in hundreds of picoseconds) in UWB allows for better spatial resolution than the narrowband counterparts. The large bandwidth also makes it possible to obtain informatin about the location and nature of one object amongst many others [XT12]. UWB radars also find use in "see-through-the- wall" precision imaging technology [Aft09].

In addition to these applications, UWB turns out to be a compelling choice for use in cognitive networks. Some of the advantages that UWB offers over narrowband standards which make it a better alternative are:

(i) *Dynamic Spectrum Allocation* : In cognitive networks, the spectrum conditions are always changing. This makes it imperative for the radio to allocate channels in a dynamic fashion. In addition to having a large bandwidth, technologies such as Impulsed Radio UWB (IR-UWB) allow for varying channel occupancy by simply changing the time-length of a pulse.

(ii) *Data Rate and Quality of Service (QoS)* : When the cognitive networks interfere with the licensed systems, the result may be the decreasing of QoS for cognitive radios. In many cases it may result in termination of network too. A solution to this problem is to dynamically change the data rate of the cognitive radio. A case in point is the IR-UWB which can make up for its lower throughput by increasing the channel bandwidth. It can achieve this capability by changing the pulse width of transmission.

(iii) *Adaptable Transmit Power* : In addition to the licensed systems, cognitive radios often have to deal with the spectral masks set-up by the regulating authorities in the concerned country. Mostly, UWB has its spectral limit set at the level of thermal noise floor. As such, by its very nature, it is adaptable to most power compliance scenarios.

(iv) *Multiple User Accessibility* : The basis of cognitive radios is the the reuse of unoccupied communication channels. This concept entails that many-users should be able to access the entire bandwidth and occupy a certain part of it. In IR-UWB, by adjusting the number of chips, the number of users can be determined.

(vi) *Information Security*: The UWB is inherently a secure mode of transmission. We have previously mentioned that the UWB spectral mask is very close to the thermal noise floor. If the radio is embedded with a directional antenna, owing to the low spectral density, it is not possible for the unwanted users to even detect the presence of signal. In addition, the IR-UWB also provides for time hopping. The data of one user can only be accessed by the other if he/she is in the know of the primary user's time-hopping sequence code.

(vii) *Cost and Complexity of Hardware*: The UWB radio inherently operates in the baseba- nd. As a result, it does away with the use of downconverters, local oscillators etc. This feature enormously brings down the implementation cost and makes cognitive radio, on a whole, a profitable solution to growing wireless congestion.

Despite all the above listed benefits, UWB radio suffers greatly from interference with other licensed standards[GZ05] (Figure 1.2). Because of the large bandwidth occupied by the standard, it inevitebly overlaps with other wireless communication standards like the WiMAX and wireless LAN (IEEE 802.11 series) . This thesis focuses on the interference from wireless LAN (WLAN) in 5-6 GHz band. From the perspective of a passive component designer, the solution to this problem lies in introducing a transmission notch in UWB filter frequency response.

The notch can be introduced either in *(a)* antennas or *(b)* filters. Various antennas with notch structures have been reported for UWB applications [RNH12][JW12]. Although the antennas offer a compact solution, here the problem lies in having selective notch-filtering in antenna's frequency response. More often than not, any tunability in the impedance charac-

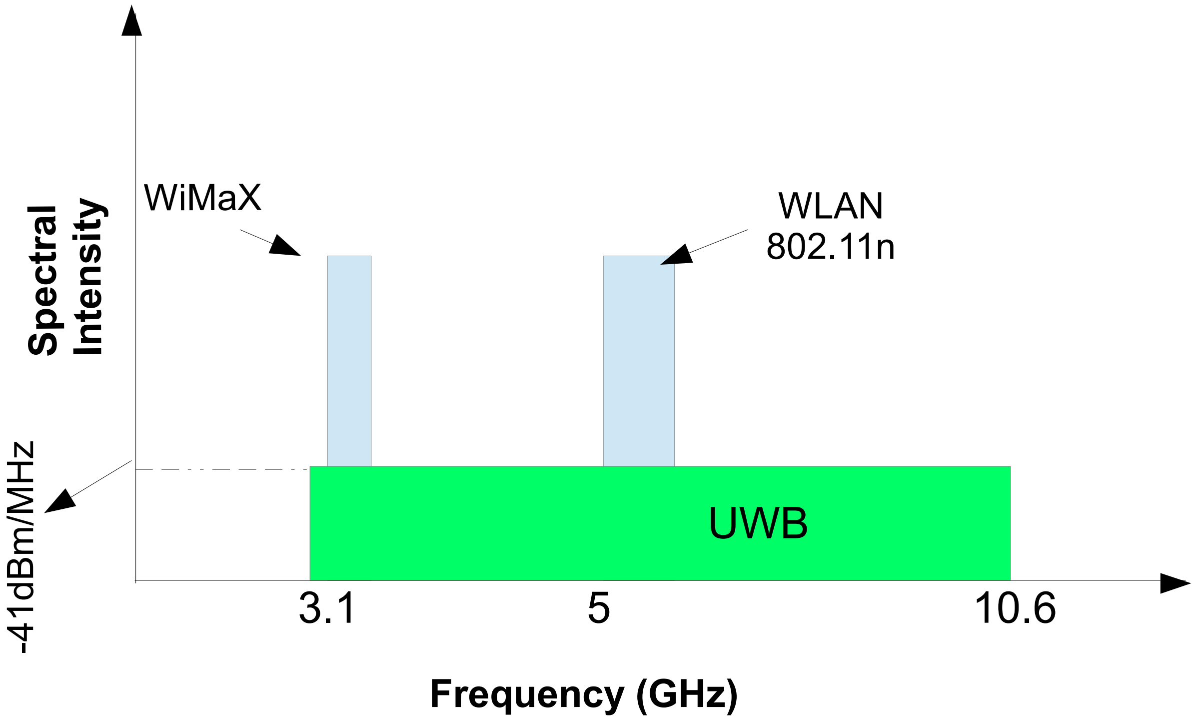

Figure 1.2: UWB with the interfering WiMAX and WLAN bands.

teristics has a detrimental effect on the radiation characteristics of the antenna. A solution to this problem lies in having an antenna with desired radiation characteristics across the UWB band followed by a tuneable notch filter to cover the WLAN band. This manuscript will detail a simple implementation of such a filter with the notch tunability across the 5-6 GHz WLAN band. An additional feature of changing bandwidth of the notch is also implemented in the same filter. The reason for introducing the capability is detailed in the following chapters.

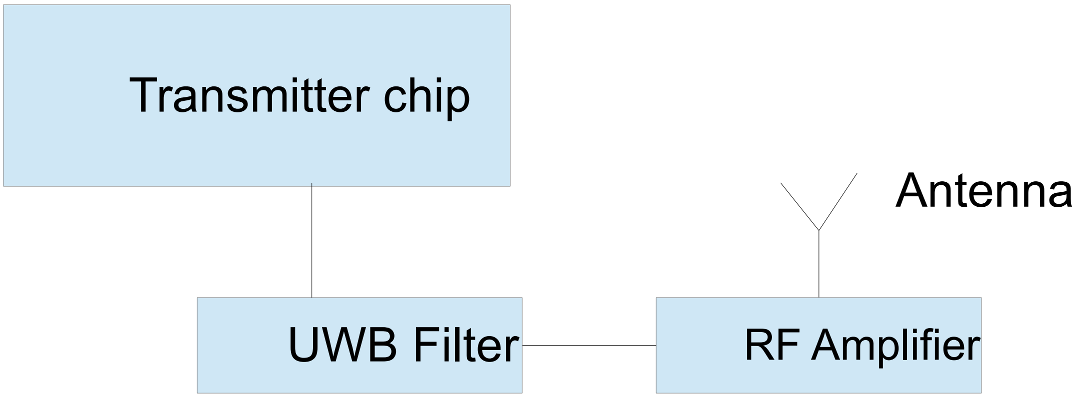

Figure 1.3: Block diagram of UWB transmitter.

1.3 Organization of The Thesis

Chapter 2 details the theory behind development of the tunable notch UWB filter.

Chapter 3 describes the implementation of DC bias circuits for the UWB notch tunability.

Chapter 4 reports the implementation of filter on dielectric substrate and subsequent test results.

Finally, **Chapter 5** concludes the thesis with some discussions on future work.

CHAPTER 2

Design of The Notch Filter

The chapter details the theoretical background behind the realization of tunable notch filter. It aims to take the reader through sequential steps of designing the UWB filter, the modification in filter geometry for introduction of the notch in frequency response and finally the addition of two indepentantly controlled notches delineating the logic behind choosing the presented topology.

2.1 Nuts and Bolts: The Ultrawideband (UWB) Filter

Even if it was not for the tremoundous incentives offered by the UWB technology, the challenge in designing an extremely wideband planar filter is reason enough to attract the attention of microwave engineers. It is a well known fact that the traditional passive filter design theory was developed for narrowband specifications [MSCnt][LM02]] rendering the theoritical design of ultrawideband filters extremely difficult. As a matter of fact, before mid-2003, the bandwidth of the bandpass filters was extended from 40-70% and these filters were termed as broad bandpass filters. That the UWB presented a bandwidth requirement of 110% (3.1 - 10.6 GHz), clearly potrays the design challenge associated with these filters.

One of the easiest ways to implement UWB filters is to cascade a high pass and an low pass filter[TC07],[WLW05]. The frequency response of these filters can also be considered as a multiplication of the individual responses of the low pass and high pass filters (if there is no matching loss). The methodology allows for good selectivity but leads to higher insertion loss and an increased circuit footprint.

Another solution is to use multiple-ring resonators to insert two transmission zeroes: one below 3.1 GHZ and the other above 10.6 GHz. The transmission zeroes relied on the resonance of narrowband ring resonators and as such, the filters suffered from narrow stopband frequency characteristics both on the upper and lower stopbands [IA04]. Also, the filter occupies a large size making its use in modern communication systems difficult.

Optimum high pass filters with short circuit stubs have also been explored for realizing a class of quasi-bandpass filters. However, the presence of vias to create shorting stubs has always been an issue for planar microwave circuits [GA06].

In a parallel development Zhu et al. introduced the concept of multiple mode resonator (MMR) [ZSM05] for attaining ultra-wideband frequency responses. Such a MMR implemented in microstrip technology is shown in Figure 2.1. The multiple-mode resonator is essentially a planar transmission line type resonator. Note that the physical topolology of multiple mode resonator is very similar to that of stepped impedance resonator (SIR) used for low pass filter design. The resonator is a symmetrical component with the middle section (Z_1) having a a low impedance continued into high impedance sections (Z_2) on both its ends. The SIR has a high impedance line section in the middle and two low impedance line sections on the two sides. For analysis purposes, let the two corresponding sections have electrical lengths of θ_1 and θ_2 respectively.

As the MMR is a symmetrical structure, it lends itself to even-odd mode analysis. By placing a short circuit at the symmetrical plane, we can do the odd mode analysis of the filter. Referring Figure 2.1, the input impedance for the odd-mode (Z_o) at the left hand termination is given as:

$$Z_o = jZ_2 \frac{Z_1 \tan\theta_1 + Z_2 \tan\theta_2}{Z_2 - Z_1 \tan\theta_1 \tan\theta_2} \tag{2.1}$$

For resonance, the condition is

$$Z_o = \infty \tag{2.2}$$

Using the above two equations we get

$$Z_2 - Z_1 \tan\theta_1 \tan\theta_2 = 0 \tag{2.3}$$

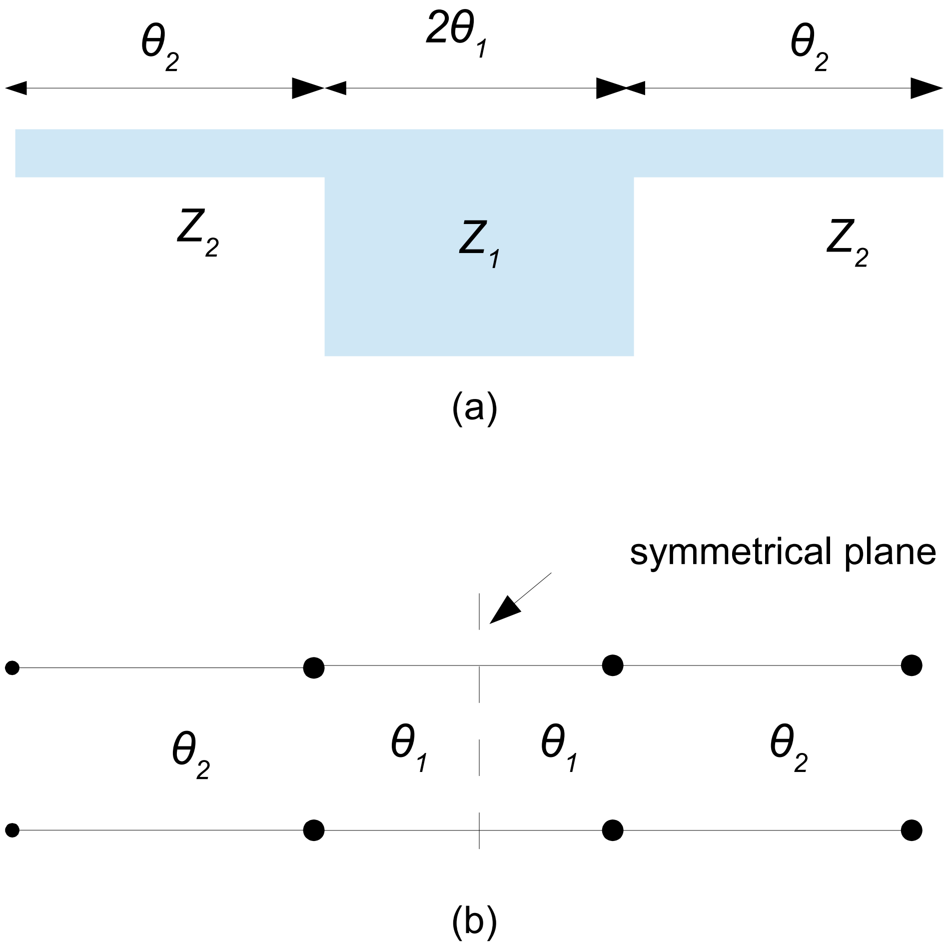

Figure 2.1: (a) Multiple-mode stepped impedance resonator (b) Transmission line equivalent model of the resonator

Now, if we assume that $\theta_1 = \theta_2 = \theta$, (2.3) becomes

$$\tan\theta = \pm\sqrt{R} \tag{2.4}$$

where $R = Z_2/Z_1$. Two frequencies can be found from equation (2.4) to give the resonance modes of the filter:

$$\theta(f_1) = \arctan\sqrt{R} \tag{2.5}$$

$$\theta(f_3) = \pi - \arctan\sqrt{R} \tag{2.6}$$

Again, the even mode impedance Z_e can be derieved by putting an open circuit at the symmetry plane as shown in Figure 2.1.

$$Z_e = jZ_2 \frac{Z_2 \tan\theta_1 \tan\theta_2 - Z_1}{Z_2 \tan\theta_1 + Z_1 \tan\theta_2} \tag{2.7}$$

Using the resonance condition

$$Z_e = \infty \tag{2.8}$$

and $\theta_1 = \theta_2 = \theta$, we get

$$\theta(f_2) = \pi/2 \tag{2.9}$$

$$\theta(f_4) = \pi \tag{2.10}$$

Assuming that the microstrip lines are non dispersive and both line sections have equal phase velocity, by $\theta \propto f$, we obtain

$$\frac{f_1}{f_2} = \frac{2\arctan\sqrt{R}}{\pi} \tag{2.11}$$

$$\frac{f_3}{f_2} = \frac{2(\pi - \arctan\sqrt{R})}{\pi} \tag{2.12}$$

$$\frac{f_4}{f_2} = \pi \tag{2.13}$$

and the normalized separation as

$$\Delta f_{13} = \frac{f_3 - f_1}{f_2} = \frac{2(\pi - 2\arctan\sqrt{R})}{\pi} \tag{2.14}$$

From the above analysis, it can be seen that first three resonance frequencies can be used to form the passband of the filter with f_2 being the mid-band frequency and separation (2.14) determining the bandwidth. It can also be seen that f_4 is always twice the mid-band frequency and is responsible for forming a higher spurious passband. Later, in Chapter 3 we would see how the DC bias circuit could take care of this problem.

Figure 2.2 shows the schematic of a MMR UWB filter with two input-output feedlines having capacitive coupling to the UWB resonator. Such couplings allows for a broad-band impedance match to the resonator. The coupling strength is directly dependant on the spacing between the resonator and the input/output feeding lines.

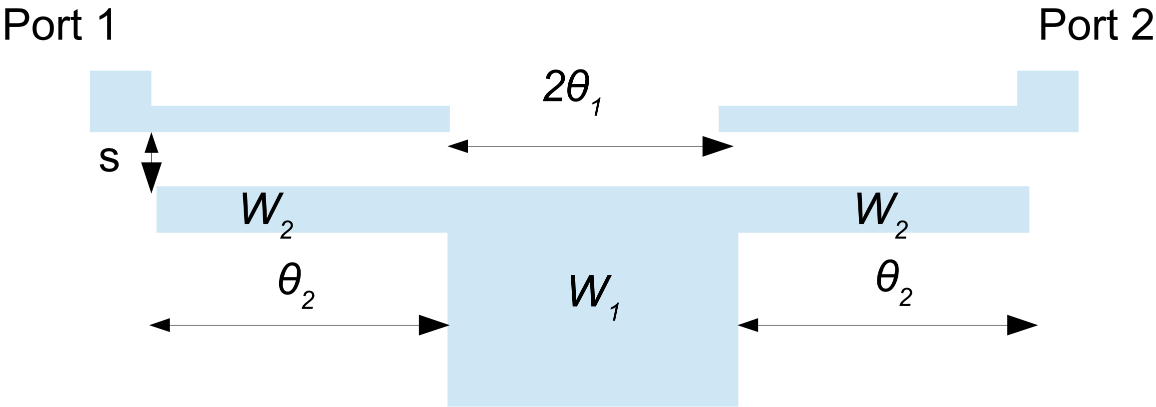

Figure 2.2: Multiple-mode stepped impedance resonator with I/O excitation lines

Figure 2.3 shows the variation of various frequency parameters calculated previously, with changing values of the impedance ratio, R[Hon11]. Figure 2.4 shows the effect of variation of the impedance ratio, R (or the ratio of section widths W_1 and W_2) on the frequency response of a UWB MMR filter (assuming $\theta = \pi/2$ at 5 GHz). The MMR filer is formed on a 0.5 mm thick dielectrc substrate having a relative dielectric constant of 3.15. It can be seen that the frequency spacing decreases with increasing W_1 (or R).

In [WZ05], a new class of broadside microstrip - coplanar waveguide (CPW) resonator filters were introduced. These filters differed from the one shown previously in the sense that they employed both sides of the printed circuit board (PCB) for signal transmission. The top layer of the circuit is a microstrip structure, which couples to a CPW structure on the bottom plane (Figure 2.5). The CPW structure in essence is again a multiple mode resonator with high impedance regions on the sides and low impedance section in the middle. The electrical lengths of the CPW resonator are similar to the corresponding electrical lengths in the microstrip counterpart. This structure offers clear benefits over the microstrip MMR structure in following two ways:

i) The broadside microstrip-CPW structure gives better coupling than the lateral coupling

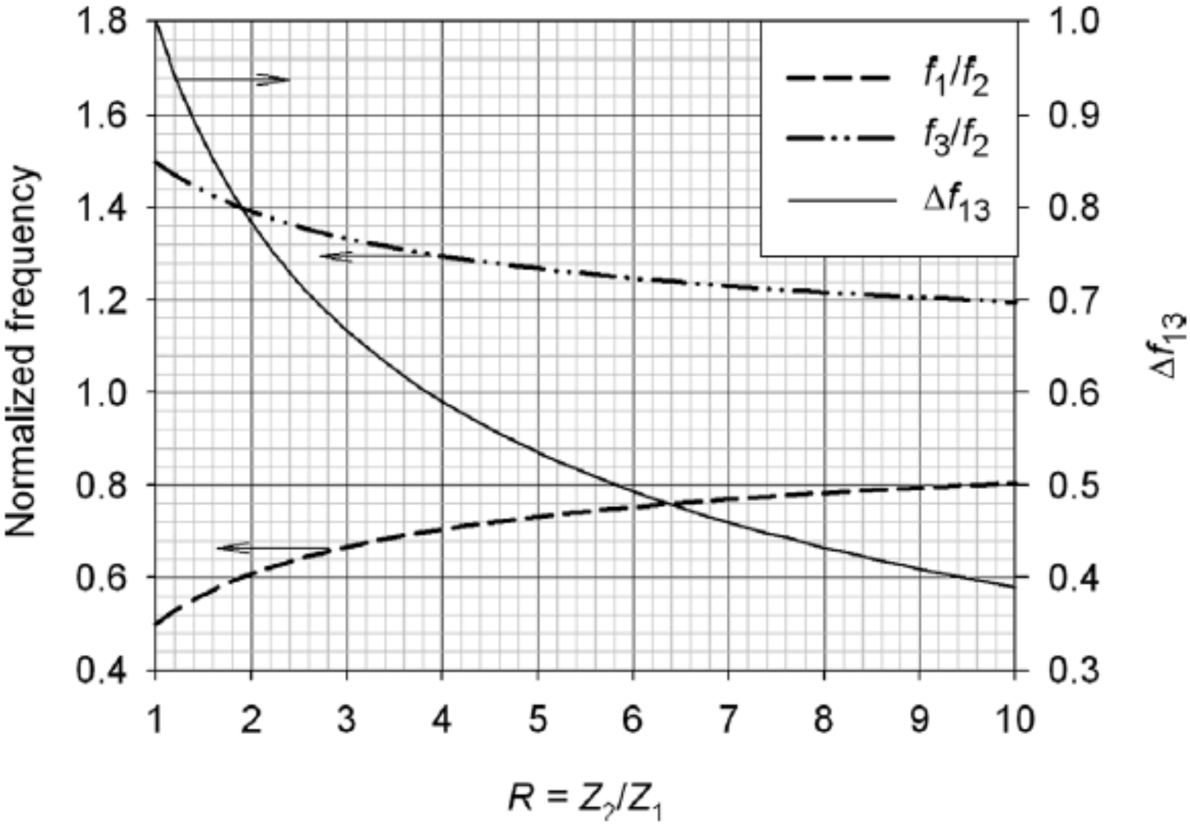

Figure 2.3: Normalized resonant frequencies and their variation with impedance ratio

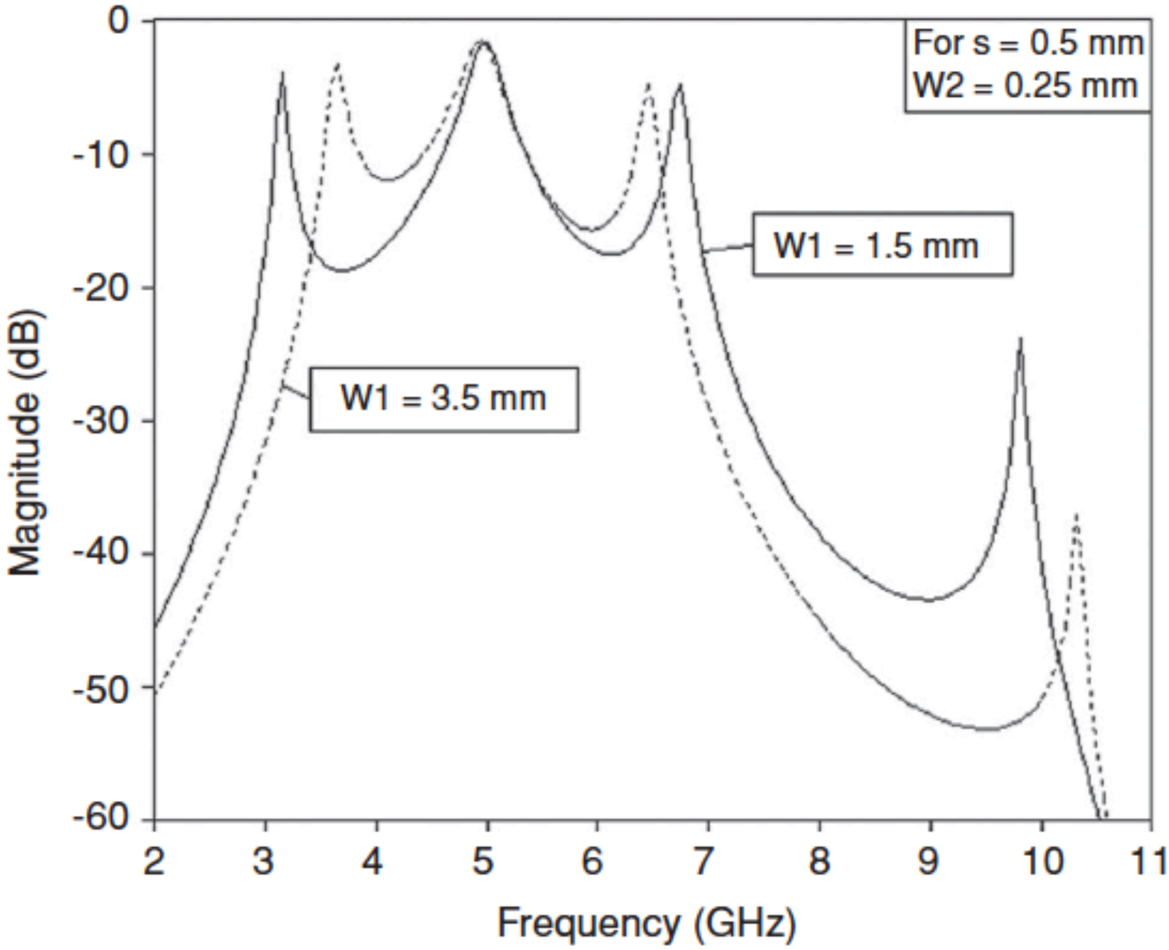

Figure 2.4: Frequency response S_{21} against the width of low-impedance line.

present in microstrip structure.

ii) There is less of spurious radiation loss from the middle section in CPW than that from the microstrip resonator.

Besides these points, there is a significant advantage of using this structure for the tunable filter design which would be discussed in the forthcoming sections.

For our simulations, we form the UWB filter on RT/Duroid 5880 LZ Laminate with relative permittivity of 1.96 and thickness equal to 0.625 mm. A planar method of moment software **Sonnet EM** is used for EM simulations. The schematic of the filter with dimensions is shown in the Figure 2.5 and the simulation results of the corresponding filter are shown in Figure 2.6.

2.2 The Notch

Notch in an UWB passband can also be viewed as trapping of travelling wave over a certain band of frequencies in the circuit so that these frequencies do not show up on the output port of the filter. Such phenomenon is generally facilitated by a resonator. The resonator can be transmission line type or its complimentary: slot type.

As we intend to obtain tunability of the notch frequency by varying varactor capacitances, the use of slot resonators is ruled out. We make use of the open ended quarter-wavelength resonator for obtaining the notch in filter S_{21} response.

An open circuited line of length l has an input impedance given by

$$Z_{in} = Z_o \frac{cot\beta l + j\tanh\alpha l}{j + \cot\beta l \tanh\alpha l} \tag{2.15}$$

where Z_o is the characteristic impedance, α is the attenuation constant and β is the phase constant of the transission line. Applying small perturbation $\Delta\omega$ at the resonant frequency and considering $l = \lambda/4$, we can write

$$\cot\beta l = \cot(\pi/2 + \pi\Delta\omega/2\omega_0) \approx \frac{-\pi\Delta\omega}{2\omega_o} \tag{2.16}$$

(a) Top plane

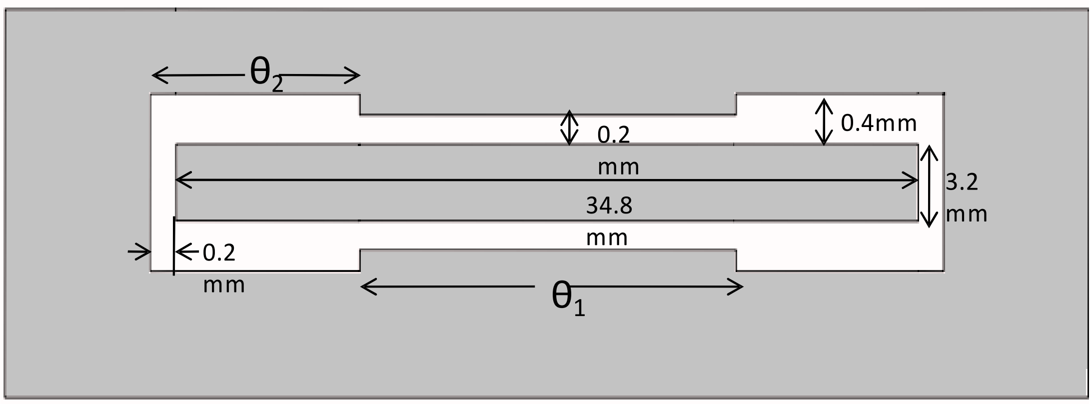

(a) Bottom plane

Figure 2.5: Broadside coupled microstrip-CPW UWB filter with dimensions.

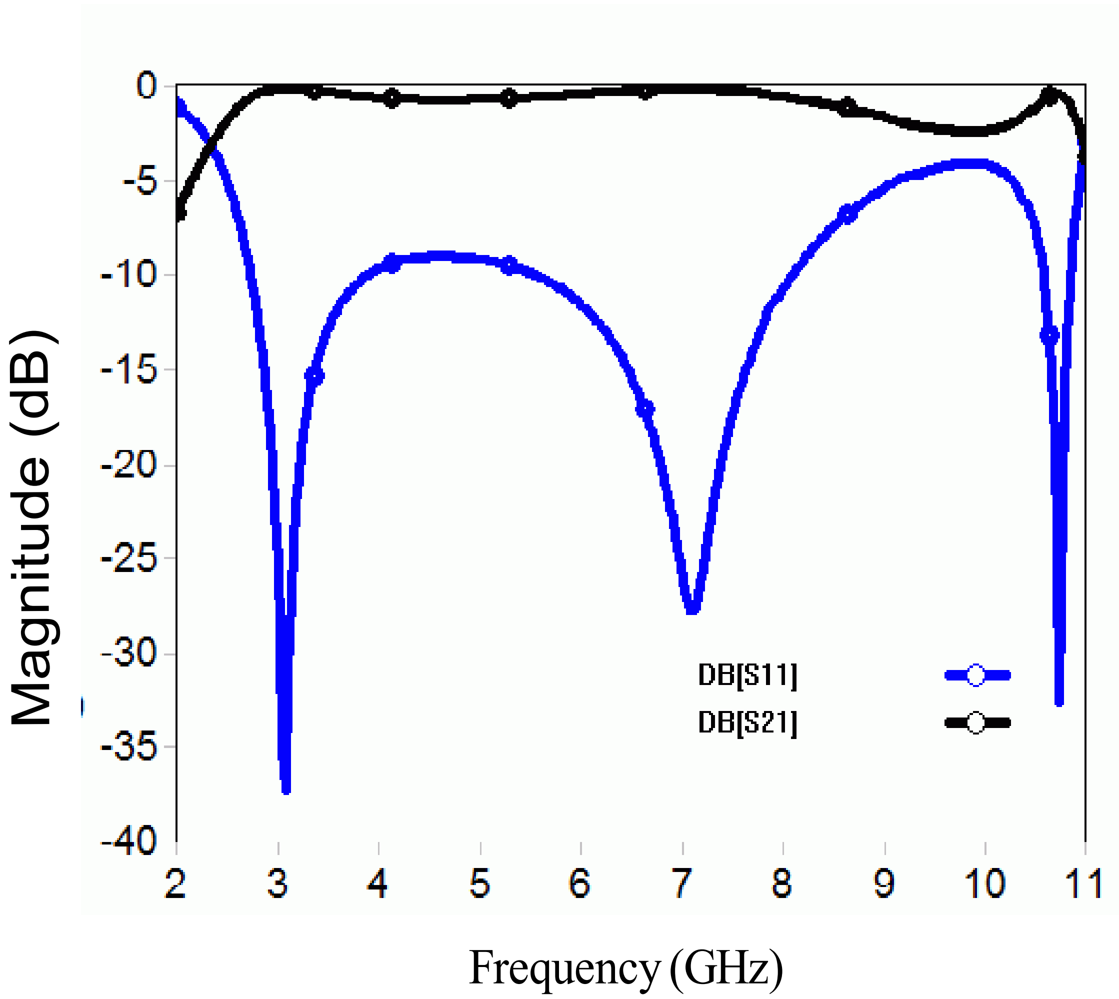

Figure 2.6: Frequency response of the microstrip-CPW UWB filter.

where ω_0 is the first resonance frequency.

Also for small loss,

$$\tanh \alpha l \approx \alpha \tag{2.17}$$

Using (2.15), (2.16) and (2.17), we can write

$$Z_{in} = Z_o(\frac{j\pi\Delta\omega}{2\omega_0} + \alpha l) \tag{2.18}$$

Comparing the above impedance to that of a perturbed series RLC resonator with $Z_i = R + 2jL\Delta\omega$ [Poz97] ,we get

$$R = Z_o \alpha l \tag{2.19}$$

and

$$L = \frac{Z_o \pi}{4\omega_o} \tag{2.20}$$

$$C = \frac{1}{\omega_o^2 L} \tag{2.21}$$

Also, for series resonant circuit the quality factor is,

$$Q = \frac{\omega_o L}{R} = \frac{1}{\omega_o C R} \tag{2.22}$$

$$Bandwidth = \frac{1}{Q} \tag{2.23}$$

The quarter wavelength notch is embedded in the microstrip structure of the broadside coupled microstrip CPW UWB filter as ashown in the Figure 2.7. Using the proposed structure in the chosen UWB filter topology has some significant advantages, namely:

i) The microstrip stub resonator is $\lambda/4$ in length at a higher frequency than WLAN range owing to its small size. Adding a capacitor in series could bring down the notch frequency in the WLAN band of 5-6 GHz.

ii) The resonators are $\lambda/2$ away from each other, which greatly reduces their electromagnetic coupling while preserving the small size of the filter.

iii) The passband of filter is because of the resonances of CPW MMR. Introducing a physical perturbation in the microstrip structure does not have a significant determintal effect on the response of filter.

Figure 2.7: Modified top plane microstrip structure.

The simulation results of the filter with the modified microstrip structure is shown in Figure 2.8. A transmission zero is clearly visible at around 10 GHz because of the $\lambda/4$ resonator.

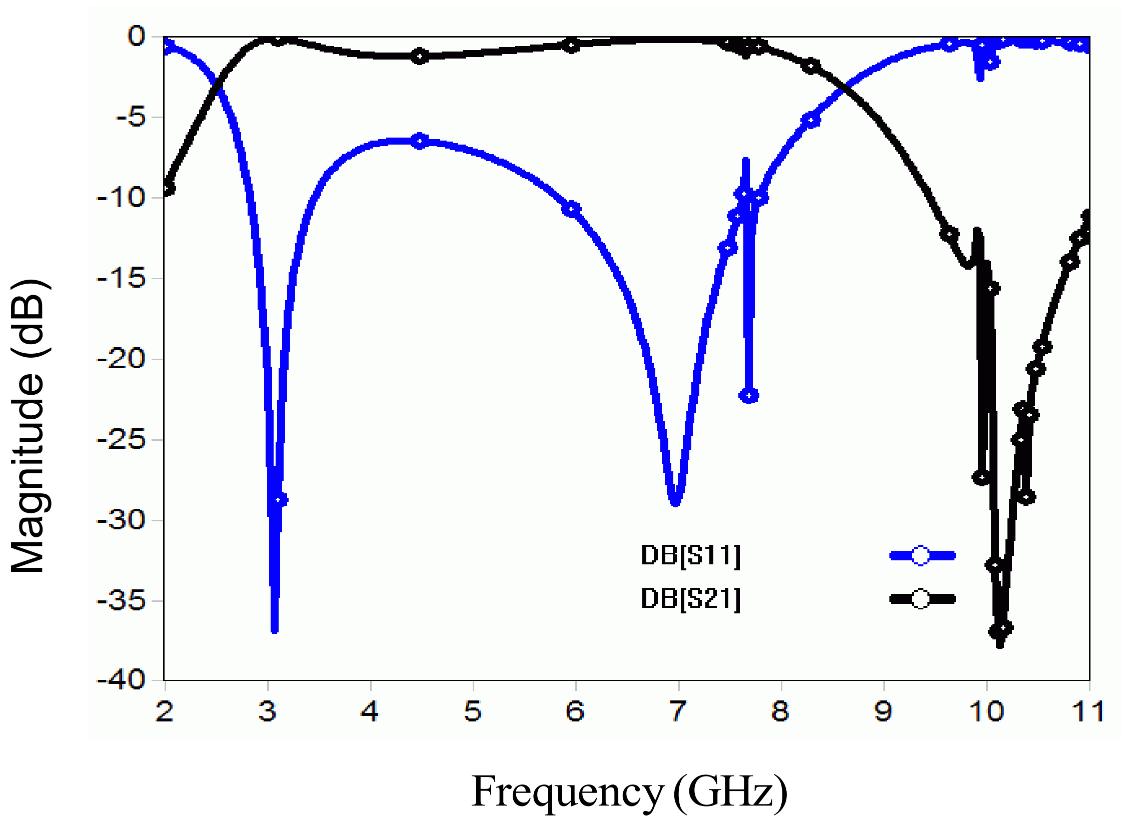

Figure 2.8: Frequency response of the filter with modified microstrip structure.

2.3 The Tuning Elements

Reconfigurability in passive microwave components is attained through electronic switching, mechanical tuning or material property tuning. Mechanical actuators are often bulky and slow in response while tunable materials suffer from lack of proper modeling, poor efficiency and reliability issues. On the other hand, electronic switching utilizes either of MEMS, PIN or semiconductor varactor diodes. The advantage of having continuously tuned capacitance coupled with lower DC current flow in comparison to MEMS and PIN diodes makes varactor diodes a good choice for achieving tunability at RF/microwave frequencies. Add to that the high control voltage and DC bias current (ON state) required for operating MEMS and PIN diodes respectively, the incentive for using varactor diodes in frequency agile microwave devices is even stronger.

Now the question arises where to place the varactors for maximum sensitivity to control voltage. The varactor in essence is a capacitor and it is known that the impact of lumped capacitor is most at the location of maximum electric field. In a quarter wavelength stub resonator, electric field maxima happens at the open end. That precisely are the locations where we use the varactors in both the microstrip sections. Because microstrip structures have small capacitances, it is imperative that we use varactors with low capacitances for greater sensitivity to bias voltage. The reason for using the varactor MA46H120 from M/A-COM is a good capacitance ratio coupled with small capacitance values (Figure 2.9)[cha]. Again, for resonance,

$$\omega_o = \frac{1}{\sqrt{LC_{eq}}} \tag{2.24}$$

where $C_{eq} = \frac{CC_v}{C+C_v}$ with C_v being the varactor capacitance and L and C the inductance and capacitance of microstrip resonator respectively.

The top plane of the modified UWB structure is shown in Figure 2.10. The fixed capacitors are 10pF DC bypass capacitors used to block the DC control voltage from flowing into the RF ports (Chapter 4). Figure 2.11 shows the variation of microstrip structure characteristic with the varactor capacitance. It can be seen that even though the matching is poor, the shift in resonant frequency due to the variable capacitance is obvious.

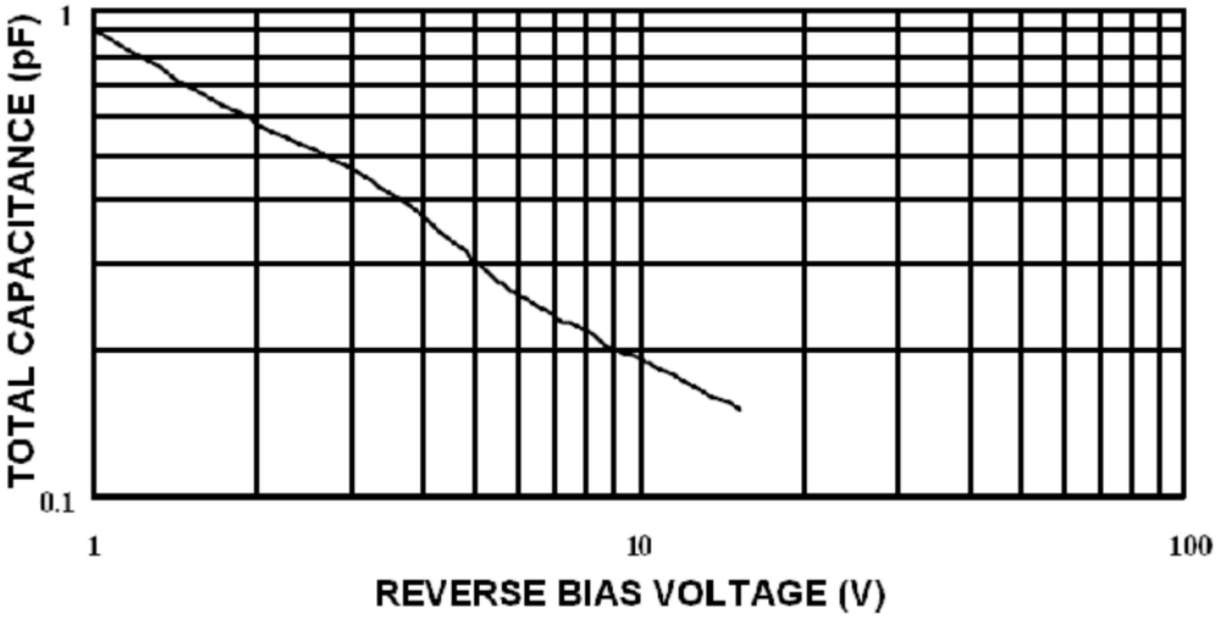

Figure 2.9: Capacitance-voltage characteristics of the M/A-COM varactor.

It is to be noted that there are two varactor controlled resonators in the filter structure. At first glance, we could say that two resonators would improve the quality factor of the notch than that of the one produced by a single resonator. This follows from the observation that the coupling between the two resonators is minimal, thus preventing the splitting of transmission zeroes. However, another major advantage of using this topology is that there is no conductor connecting the two resonators. This should allow for independant tuning of the two resonators, thus supporting the variation in notch bandwidth with a tradeoff in quality factor of the notch. The above point would be further elaborated in coming chapters.

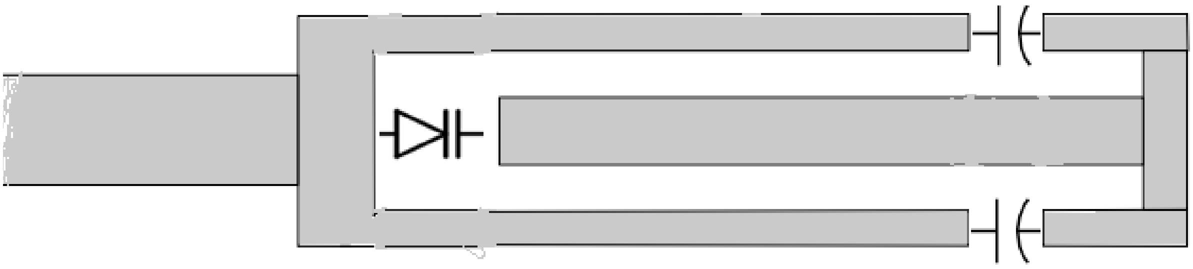

Figure 2.10: Modified top plane microstrip structure.

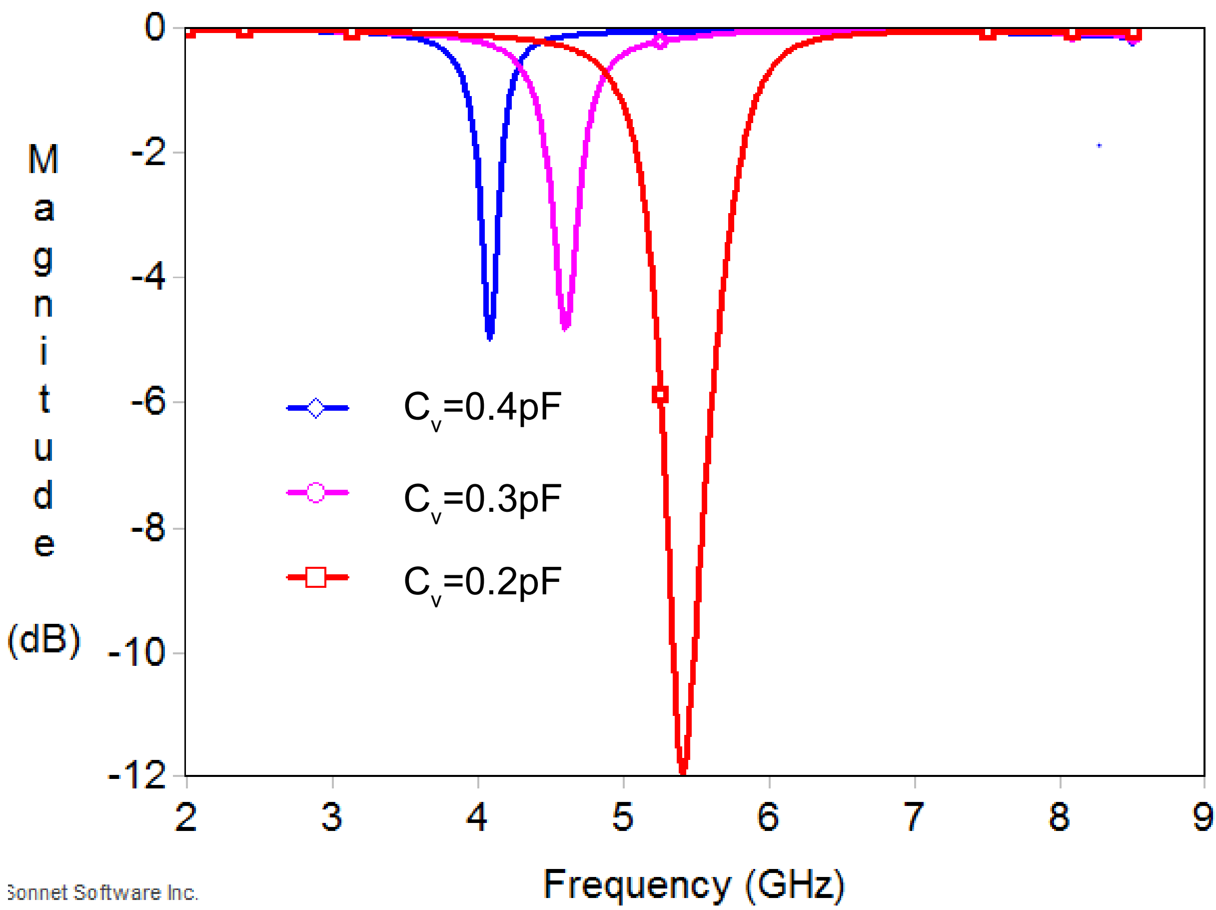

Figure 2.11: Effect of varactor value change in microstrip structure on S_{11} values.

CHAPTER 3

The Control Elements: DC Bias Circuitry

An important part in the development of tunable passive components is to provide it with the appropriate bias circuit for manipulation of agile components. A good DC bias circuitry for tunable filters is one which provides open circuit to the filter across its passband, so that no travelling waves from the passband frequencies escape into the bias circuitry. For UWB this frequency ranges from 3.1 to 10.6 GHz. If this is not a challenge enough, the limitation of self-resonance frequencies of lumped components inhibits their use at higher frequencies. In essence, the ideal DC bias circuitry should be a stopband filter from 3.1 to 10.6 GHz with phase response of reflection coefficient at 0 degrees across the UWB frequency range.

A fully distributed DC bias circuitry is implemented as shown in Figure 3.1. The fan stubs used are again quarter-wavelength resonators with a wider bandwidth than their stub counterparts. At their input ports these fan stubs present a short circuit, so they are provided by $\lambda/4$ transmission lines to invert the impedance into an open circuit. It is interesting to note that the narrower these lines get, better do the stopband characteristics. The resolution limit available to us was 0.1 mm, hence the transmission line width in Figure 3.1. Sonnet EM is used to optimize the structure so that a DC bias circuitry is obtained for UWB range. The frequency response on a smith chart is shown in Figure 3.2.

An interesting point to note from the above chart is that the impedance moves from open to short for higher frequencies. Recall that the fourth resonance frequency of the MMR resonator (2.10) is responsible for providing a spurious passband above the UWB frequency range. If designed carefully, the short circuit characteristics of the DC bias circuitry at these fequencies can be used to ground the travelling wave. Thus, the DC bias circuit not only is an enabler of tunability in the filter response but also improves the stopband characteristics of the UWB filter.

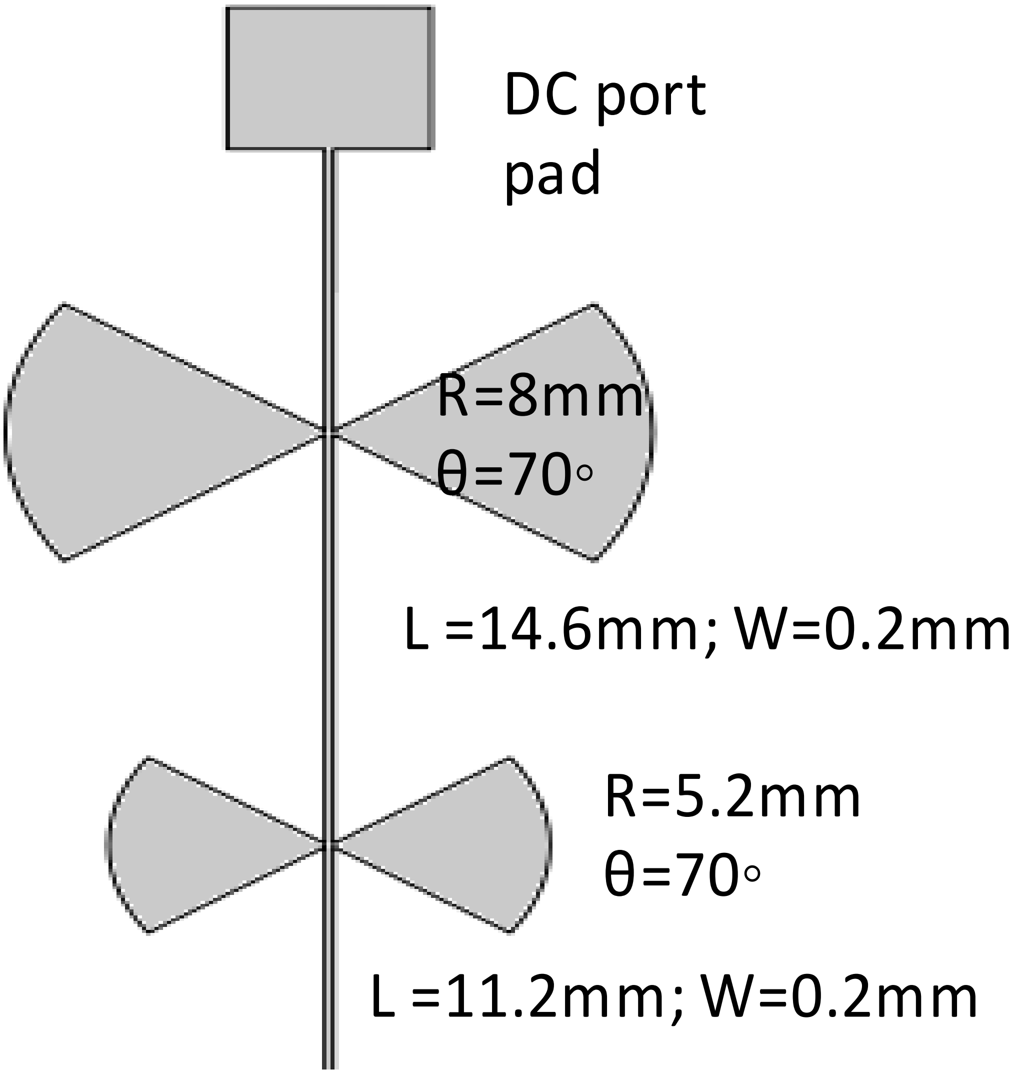

Figure 3.1: DC bias circuitry.

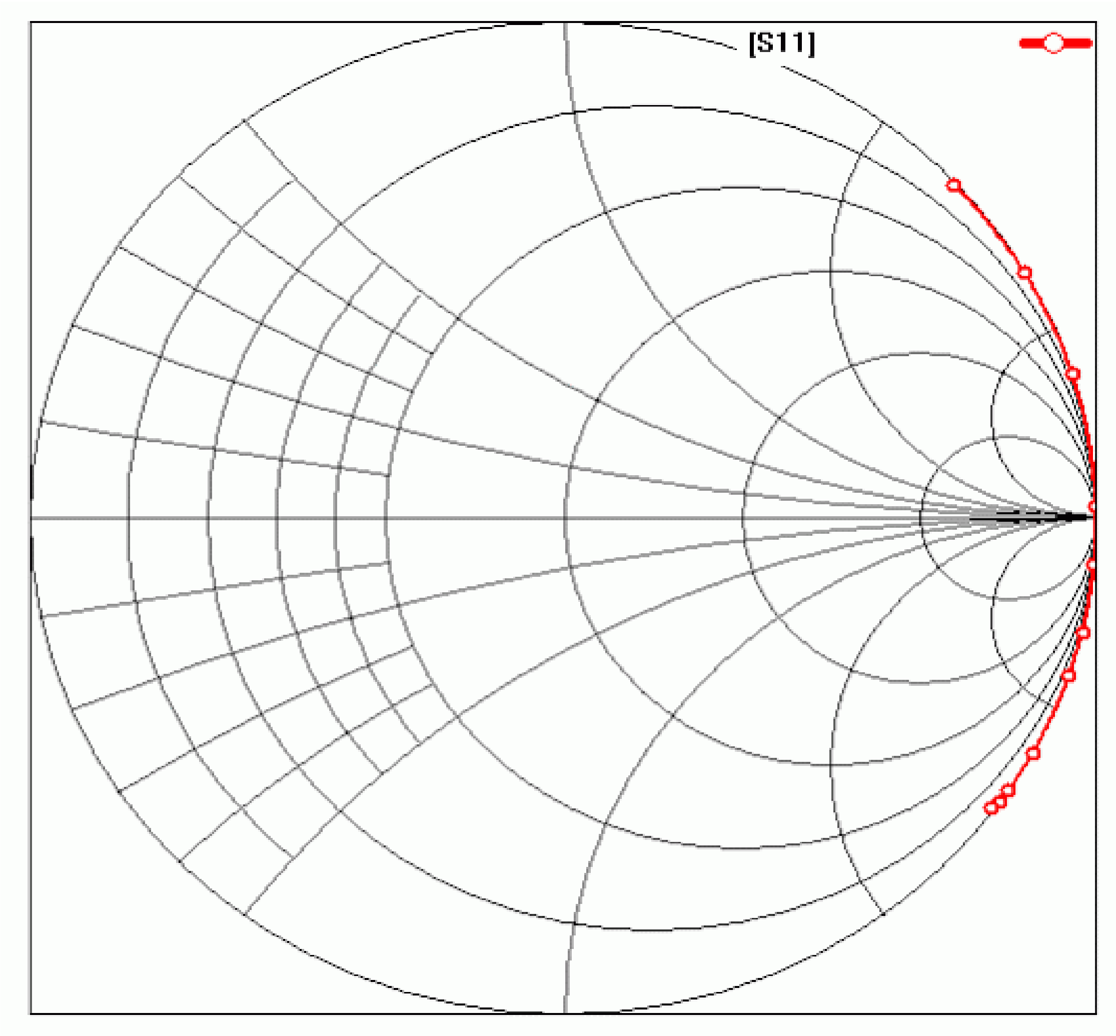

Figure 3.2: Frequency response of the DC bias circuitry for 3-8 GHz.

CHAPTER 4

Implementation and Results

The filter is fabricated using the standard PCB process. Bias circuits are applied to both the microstrip sections as shown in Figure 4.1. This is done to enable independant tuning of both the varactor loaded resonators. A pair of DC by-pass capacitors are used on each microstrip section to block the DC voltage from passing into the RF I/O ports. The bottom plane is shown in Figure 4.2.

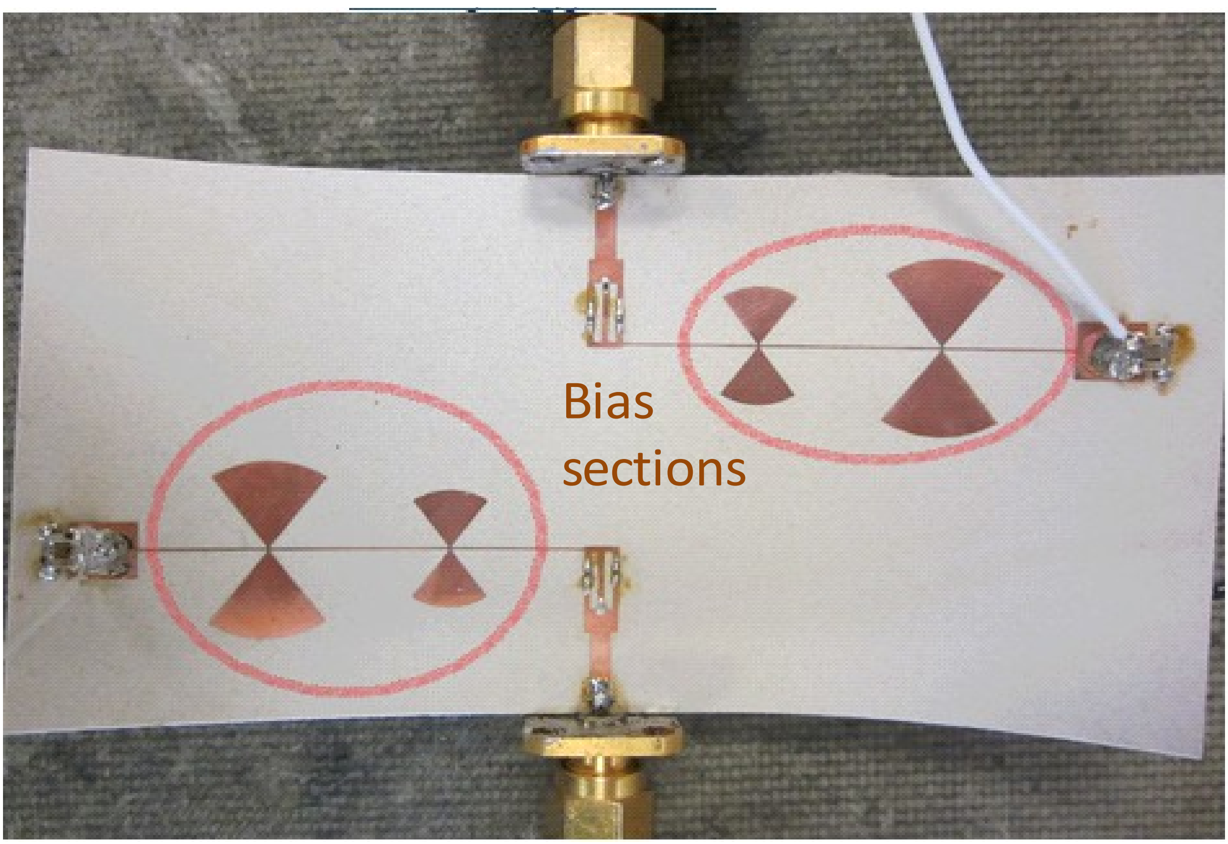

Figure 4.1: Top plane of fabricated filter.

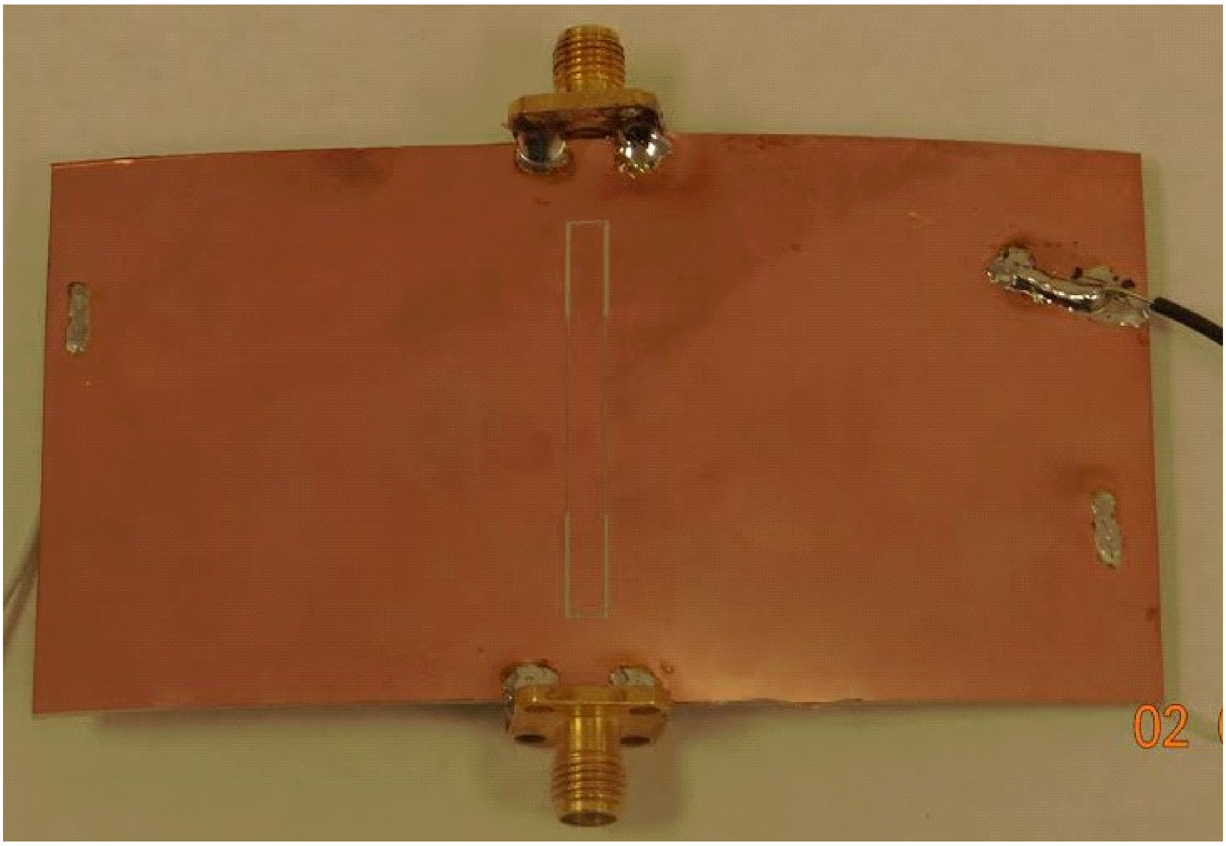

Figure 4.2: Bottom plane of fabricated filter.

Initially, both the bias circuits are fed by a single voltage source. Agilent 8510C vector network analyzer is used for testing the filter. A reference impedance of 50Ω is used for calculating the filter characteristics. Figure 4.3 shows the measured variation of notch frequency with the change in DC voltage. It can be seen that the notch frequency increases with the applied voltage. This is because the value of C_v goes down with increasing reverse-bias voltage and as such, by (2.24) the resonant frequency ω_0 increases. Again, by (2.22), quality factor of the notch increases and the notch becomes sharper with increasing voltage. It is observed that the notch is able to span across the entire 5-6 GHz band on variation of bias voltage from 8V to 19V. Rejection levels of more than 15 dB are observed in the WLAN band. The passband is shifted to lower frequencies (2.5 GHz) but still maintains an equivalent UWB (109.5%) bandwidth. The shifting can be ascribed to fabrication tolerances. The insertion loss remains below 1 dB, but is somewhat higher between 3 to 4 GHz.

This may be attributed to the presence of notch structure and the bias network. Another observation is that the deteriorating phase characteristics of the DC bias network beyond 8 GHz (Figure 3.2) can serve to greatly improve the upper stopband characteristics of the MMR UWB filter.

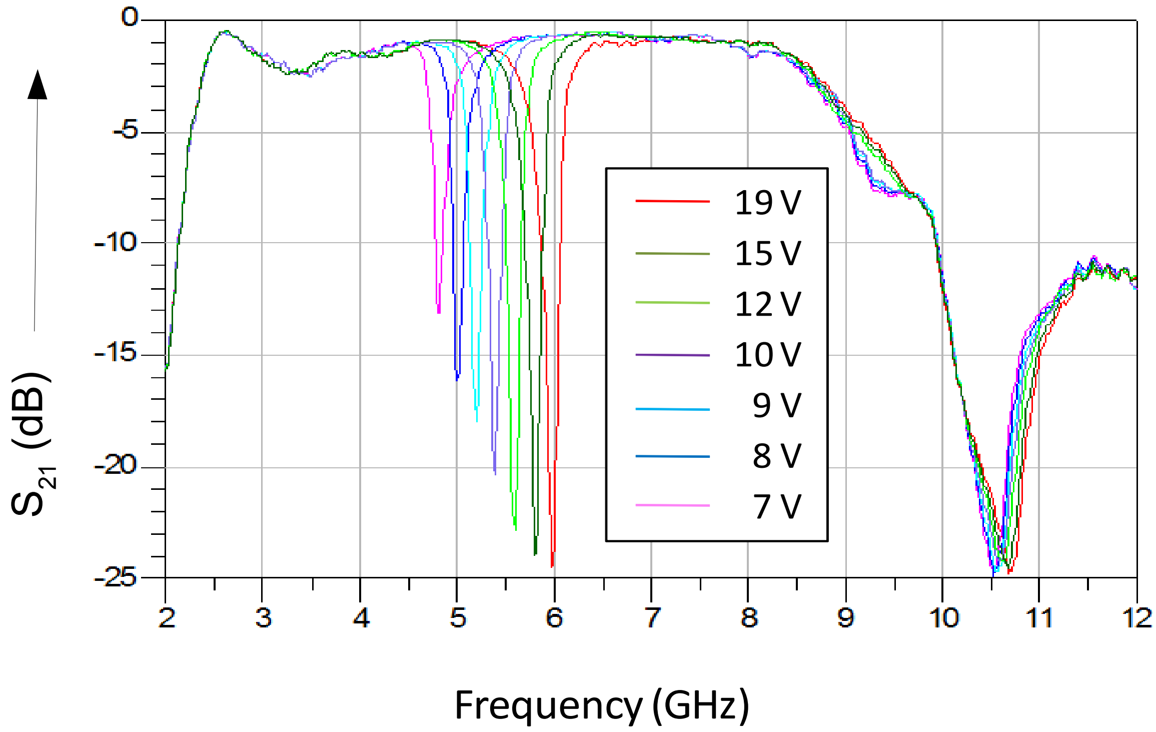

Figure 4.3: Measured frequency response of the filter showing tunability of the notch with change in bias voltage.

It is known that the channels in WLAN (5-6 GHZ) band have the same bandwidth allocation. So, it is important for the notch to be able to maintain this bandwidth as the notch is being tuned. Because bandwidth = $1/Q$ and Q is dependant on varactor capacitance C_v, bandwidth of the notch is a function of bias voltage V.

Put succintly, for maintaining constant bandwidth, the filter should be embedded with bandwidth tunability. As discussed in the previous chapter, the presence of two independantly controlled resonators which have minimal couupling allows us to do so. For this purpose, each of the bias circuitry is controlled by a different voltage source. Let these source voltage be V_1 and V_2. Figure 4.4 shows the presence of constant 10 dB bandwidth of 150 MHz for varying notch frequencies.

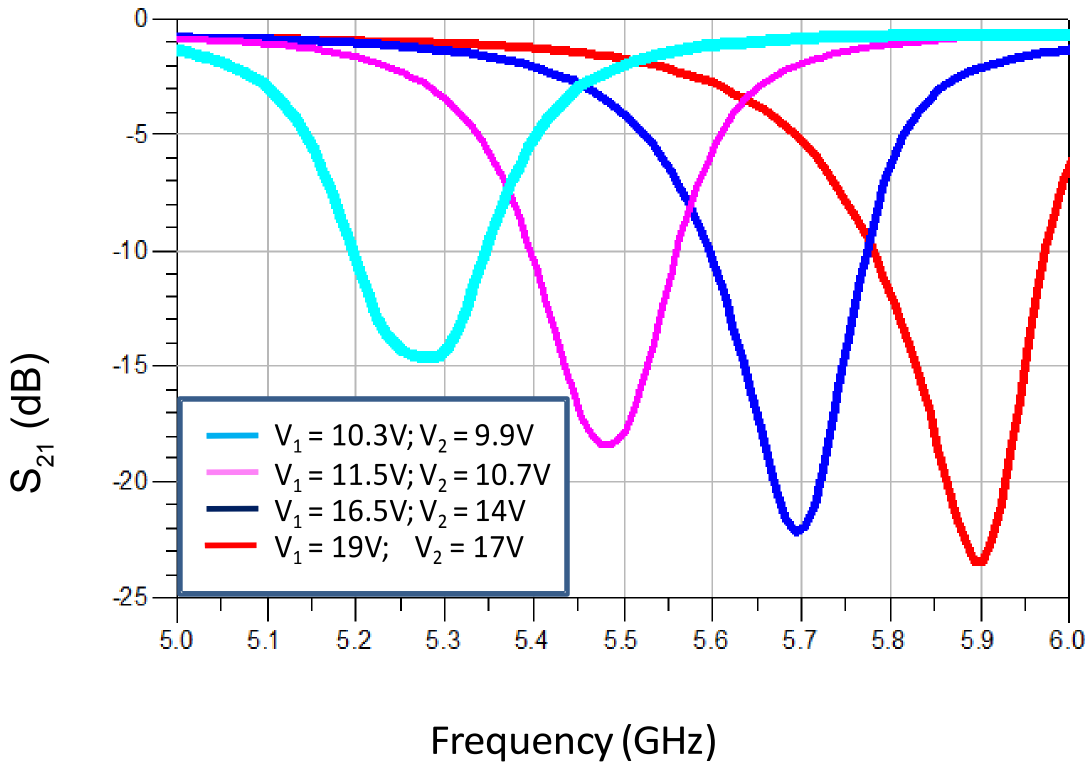

Figure 4.4: Constant notch-bandwidth tunability of filter.

CHAPTER 5

Conclusion and Future Prospects

5.1 Conclusion

A novel reconfigurable UWB notch filter has been presented. The filter is a multiple mode resonator with a length of one-wavelength at the mid-band frequency. Three resonant modes of the CPW MMR are used for creating the passband while microstrip structure is used for coupling the RF signals to MMR. A tunable notch is obtained in the frequency response by embedding varactor loaded stubs in the microstrip structures of the filter. Rejection levels of more than 15 dB are obtained across the tuning range of 5-6 GHz, which happens to be the interfering WLAN band. The ability to control both the varactors independantly allows for tunable bandwidth of the notch.

5.2 Future prospects

Simultaneous advantages like low atmospheric attenuation, ability to form narrow beams and practical antenna size means the UWB band would become all the more congested with time. For the filter to be used in cognitive radio and be fully accomodative of modern wireless communication systems, the notch should be able to tune across the UWB band. Considering that low-priced, commercial semiconductor varactors wouldn't be increasing their capacitance ratio drastically in coming years, it is imperative to increase the sensitivity of the circuit to varactor capacitance change. It is known that the resonant frequency of the notch is given by:

$$\omega_o = \frac{1}{\sqrt{LC_{eq}}} \tag{5.1}$$

where $\frac{1}{C_{eq}} = \frac{1}{C_v} + \frac{1}{C}$ with C_v being the varactor capacitance and L and C the inductance and capacitance of microstrip resonator respectively. It could be observed from the above equations that large value of resonator capacitance C makes the notch frequency more sensitive to bias voltage change. Development of compact resonators with $C \approx 10^{-11}$ Farads and $L \approx 10^{-9}$ Henry is critical for UWB notch tunability.

Another method to achieve notch tunability across the UWB band (Bandwidth: BW) is to make the two stub resonators span complimentary frequency ranges. Let's say one of the tunable notch is able to span a frequency range R_1 , then the other notch should be able to cover the remaining frequency range. That is, its frequency spanning range should be BW - R_1. Thfilter presented in this thesis is useful for this purpose, as both the resonators can be independantly tuned. The major challenge here is to design compact notch producing resonators with very high quality factors. A trade-off with this approach is the loss of bandwidth tunability.

References

[Aft09] Michal Aftanas. *Through-Wall Imaging with UWB Radar System.* PhD thesis, Technical University of Kosice, 2009.

[cha] *MA46H120 data sheet.*

[CNM14] W.J. Chappell, E.J. Naglich, C. Maxey, and A.C. Guyette. "Putting the Radio in Software-Defined Radio: Hardware Developments for Adaptable RF Systems." *Proceedings of the IEEE*, **102**(3):307–320, 2014.

[for02] FCC spectrum policy task force. "Report of the spectrum efficiency working group." Technical report, FCC, 2002.

[GA06] R. Gomez-Garcia and J.I. Alonso. "Systematic Method for the Exact Synthesis of Ultra-Wideband Filtering Responses Using High-Pass and Low-Pass Sections." *Microwave Theory and Techniques, IEEE Transactions on*, **54**(10):3751–3764, 2006.

[GZ05] Fabrizio Granelli and Honggang Zhang. "Cognitive ultra wide band radio: a research vision and its open challenges." In *2nd International Workshop on Networking with Ultra Wide Band (NEUWB2), Rome*, pp. 55–59, 2005.

[HL08] Shao Ying Huang and Yee Hui Lee. "Development of ultra-wideband (UWB) filters." *General Assembly of the International Union of Radio Science*, 2008.

[Hon11] Jia-Sheng Hong. *Microstrip Filters for RF/Microwave Applications, Second Edition.* John Wiley & Sons, 2011.

[IA04] H. Ishida and K. Araki. "Design and analysis of UWB band pass filter with ring filter." In *Microwave Symposium Digest, 2004 IEEE MTT-S International*, volume 3, pp. 1307–1310, 2004.

[JW12] Xiupu Zhang Jie Xu, Dongya Shen and Ke Wu. "A Compact Disc UltrawideBand (UWB) Antenna With Quintuple Band Rejections." *Antennas and Wireless Propagation Letters, IEEE*, **11**:1517–1520, 2012.

[LM02] Snyder R.V. Levy, R. and G. Matthaei. "Design of microwave filters." *Microwave Theory and Techniques, IEEE Transactions on*, **50**:783–793, 2002.

[Mit95] J. Mitola. "The software radio architecture." *Communications Magazine, IEEE*, **33**(5):26–38, May 1995.

[Mit00] J. Mitola. *Cognitive Radio: An integrated agent architecture for software defined radio.* PhD thesis, Royal Institute of Technology (KTH), Stockholm, 2000.

[Mit06] J. Mitola. *Cognitive Radio Architecture.* John Wiley, New York, 2006.

[MSCnt] George L Matthaei, BM Schiffman, EG Cristal, and LA Robinson. "Microwave Filters and Coupling Structures." Technical report, 1963, DTIC Document.

[Poz97] David M. Pozar. *Microwave engineering*. Wiley, 1997.

[RB10] E. G. Ryen and C. Babbitt. "Identifying barriers to efficient recovery and sustainable end of life management of electronic waste." In *Sustainable Systems and Technology (ISSST), 2010 IEEE International Symposium on*, pp. 1–1, 2010.

[RNH12] M. Rahanandeh, A.S. Noor Amin, M. Hosseinzadeh, P. Rezai, and M.S. Rostami. "A Compact Elliptical Slot Antenna for Covering Bluetooth/WiMAX/WLAN/ITU." *Antennas and Wireless Propagation Letters, IEEE*, **11**:857–860, 2012.

[RO02] First Report and Order. "Revision of Part 15 of the Commission's Rules Regarding Ultra-Wideband Transmission Systems." Technical report, Federal Communications Commission, 2002.

[Sol13] Office of Solid Waste. "Municipal solid waste in the United States: 2011 facts and figures." Technical report, U.S. Environmental Protection Agency, 2013.

[TC07] Ching-Wen Tang and Ming-Guang Chen. "A Microstrip Ultra-Wideband Bandpass Filter With Cascaded Broadband Bandpass and Bandstop Filters." *Microwave Theory and Techniques, IEEE Transactions on*, **55**(11):2412–2418, 2007.

[Wan09] Wei Wang. *Cognitive Radio Systems*. Intech Open, 2009.

[WLW05] Wei-Ting Wong, Yo-Shen Lin, Chi-Hsueh Wang, and Chun Hsiung Chen. "Highly selective microstrip bandpass filters for ultra-wideband (UWB) applications." In *Microwave Conference Proceedings, 2005. APMC 2005. Asia-Pacific Conference Proceedings*, volume 5, pp. 2850–2853, 2005.

[WZ05] H. Wang and L. Zhu. "Ultra-wideband Bandpass Filter Using Back-to-back Microstrip-to-CPW Transition Structure." *Electronics Letters*, **41**(24):1337–1338, 2005.

[XT12] Anh Dinh Xubo Wang and Daniel Teng. *Ultra Wideband - Current Status and Future Trends*. Intech Open, 2012.

[ZSM05] Lei Zhu, Sheng Sun, and Wolfgang Menzel. "Ultra-wideband (UWB) bandpass filters using multiple-mode resonator." *Microwave and Wireless Components Letters, IEEE*, **15**(11):796–798, 2005.